

Limits on a population of collisional-triples as progenitors of Type-Ia supernovae

Na’ama Hallakoun^{*} and Dan Maoz

School of Physics and Astronomy, Tel-Aviv University, Tel-Aviv 6997801, Israel

Accepted XXX. Received YYY; in original form ZZZ

ABSTRACT

The progenitor systems of Type-Ia supernovae (SNe Ia) are yet unknown. The collisional-triple SN Ia progenitor model posits that SNe Ia result from head-on collisions of binary white dwarfs (WDs), driven by dynamical perturbations by the tertiary stars in mild-hierarchical triple systems. To reproduce the Galactic SN Ia rate, at least $\sim 30 - 55$ per cent of all WDs would need to be in triple systems of a specific architecture. We test this scenario by searching the *Gaia* DR2 database for the postulated progenitor triples. Within a volume out to 120 pc, we search around *Gaia*-resolved double WDs with projected separations up to 300 au, for physical tertiary companions at projected separations out to 9000 au. At 120 pc, *Gaia* can detect faint low-mass tertiaries down to the bottom of the main sequence and to the coolest WDs. Around 27 double WDs, we identify zero tertiaries at such separations, setting a 95 per cent confidence upper limit of 11 per cent on the fraction of binary WDs that are part of mild hierarchical triples of the kind required by the model. As only a fraction (likely ~ 10 per cent) of all WDs are in < 300 au WD binaries, the potential collisional-triple progenitor population appears to be at least an order of magnitude (and likely several) smaller than required by the model.

Key words: binaries: visual – white dwarfs – supernovae: general

1 INTRODUCTION

A major unsolved puzzle in astrophysics is the identity of the progenitors of Type-Ia supernovae (SNe Ia; see Maoz et al. 2014; Livio & Mazzali 2018; Wang 2018, for a review). A number of progenitor scenarios have been considered over the years. Among them, several have involved the collision of two white dwarfs (WDs) in a variety of configurations and environments (e.g. Benz et al. 1989; Thompson 2011). In particular, Katz & Dong (2012) and Kushnir et al. (2013) have proposed that SNe Ia result from head-on collisions of WDs in “mild-hierarchical” triple systems. The triple system consists of an inner double-WD binary with separation $a \lesssim 300$ au, orbited by a roughly solar-mass tertiary star in an orbit with pericentre separation $\sim 3 - 10$ times the inner-binary’s separation. Using numerical integration of the evolution of such 3-body systems and assuming a uniform distribution of inclinations, Katz & Dong (2012) found that, in about 5 per cent of all such systems (the 5 per cent within a small range around a high inclination between the inner and outer orbits), the outer tertiary stochastically drives a Kozai-Lidov perturbation of the inner pair’s orbital eccentricity. Within a few Gyr, the eccentricity lands on a high-enough value to send the inner pair on a head-collision. Given that the actual distribution of inclinations of the systems that survive as a wide double WD with a tertiary companion is unlikely to be uniform, this 5 per cent is most likely an

upper limit of the fraction of systems that undergo a collision. Kushnir et al. (2013) showed that the compression undergone by the WDs upon collision could be effective both at igniting a thermonuclear carbon detonation, and in producing about $0.5 M_{\odot}$ of radioactive ^{56}Ni in the explosion, as observed in typical SN Ia events. The range of masses of the WDs that collide could also reproduce the observed range of SN Ia luminosities and their correlation with light-curve evolution time. The asymmetry of the system at the time of explosion predicts double-peaked emission line profiles in SN Ia spectra during the nebular phase in a fraction of events, for which there may be some observational evidence (Dong et al. 2015, 2018; Kollmeier et al. 2019; Vallely et al. 2019).

However, a major challenge for the collisional-triple model is to produce a collision rate that can match the SN Ia rate in our Galaxy. The Milky Way, if it is a typical Sbc galaxy, has a SN Ia rate per unit stellar mass of $(1.12 \pm 0.35) \times 10^{-13} \text{ yr}^{-1} M_{\odot}^{-1}$ (Li et al. 2011; Graur et al. 2017).¹ The stellar mass density in the Solar neighborhood is $0.085 \pm 0.010 M_{\odot} \text{ pc}^{-3}$ (McMillan 2011), and the WD number density is $0.0045 \pm 0.0004 \text{ pc}^{-3}$ (Hollands et al. 2018), giving a stellar-mass to WD number ratio of $18.9 \pm 2.8 M_{\odot} \text{ WD}^{-1}$.

¹ For a total stellar mass of $(6.4 \pm 0.6) \times 10^{10} M_{\odot}$ (McMillan 2011), the Galactic rate is $(7.2 \pm 2.3) \times 10^{-3} \text{ yr}^{-1}$, or a SN Ia every 100 – 200 yr. This is broadly consistent with the four known Galactic events over the last millennium that were likely or certain SNe Ia (SN1006, SN1572-Tycho, SN1604-Kepler, and G1.9+03).

^{*} E-mail: naama@wise.tau.ac.il (NH)

The SN Ia rate per WD is therefore $(2.1 \pm 0.7) \times 10^{-12} \text{ yr}^{-1}$, and the fraction of all WDs that explode as SNe Ia during the 10 Gyr-lifetime of the Galaxy is (2.1 ± 0.7) per cent. Considering then, that in the collisional-triple model at most 5 per cent of suitable triple systems undergo a SN Ia inducing collision, implies that at least $\sim 30 - 55$ per cent of all WDs need to be in suitable triple systems, if this mechanism is to explain all SNe Ia (see also [Papish & Perets 2016](#)).

While the observational picture on stellar multiplicity is far from clear yet, and even more so the situation regarding the multiplicity of stellar remnants such as WDs, there are already question marks as to the plausibility of such a high frequency of triples with a specific architecture [$a < 300 \text{ au}$, $r_{\text{peri,out}} = (3 - 10)a$]. The fraction of triple stars (of all configurations) among main-sequence A-through-K type stars has been estimated at 5–15 per cent ([Tokovinin et al. 2008](#); [Duchêne & Kraus 2013](#); [Tokovinin 2014](#); [Leigh & Geller 2013](#), and references therein), or 15–30 per cent ([Moe & Di Stefano 2017](#)), and likely only a fraction of those have the required architectures. [Klein & Katz \(2017\)](#) estimated the occurrence frequency of the inner binary WD component of the collisional-triple model, by analysing two published studies of $> 1 M_{\odot}$ stars (that will eventually evolve into WDs): an adaptive optics survey of A stars by [De Rosa et al. \(2014\)](#), in which $> 1 M_{\odot}$ companions within 400 au were searched for; and a radial-velocity survey by [Mermilliod et al. \(2007\)](#) of $> 1 M_{\odot}$ giants, which was searched for $> 1 M_{\odot}$ companions within 3 au. [Klein & Katz \(2017\)](#) conclude that 15–20 per cent of the intermediate mass stars that become WDs are in binaries that can constitute the inner component of collisional-triple systems, and therefore even if all such binaries had a mild hierarchical tertiary, there would still be a factor 2 shortage of collisional-triple progenitors for SNe Ia. Even if triple main-sequence systems are abundant, a challenge of the model that was already acknowledged by [Katz & Dong \(2012\)](#) is that triple systems with the suitable architecture and relative orbital inclination to induce to a collision of the inner binary will undergo such a collision already when the stars are on the main sequence (without an ensuing SN Ia), effectively eliminating all the SN Ia progenitor systems. This conclusion has emerged also from binary population synthesis calculations ([Hamers et al. 2013](#); [Toonen et al. 2018](#)). [Katz & Dong \(2012\)](#) raised the possibility that angular momentum loss by the system due to asymmetric mass loss during the evolution to the WD stage, or perturbations by passing stars, could “reset” the relative orbital inclinations of the system, and thus solve the problem.

In this paper, we address more directly the subject of the putative triple-progenitor population of SNe Ia, by searching the *Gaia* DR2 database ([Gaia Collaboration et al. 2016, 2018a](#)) specifically for double WDs orbited by a tertiary star, as envisaged in the collisional-triple model.

2 GAIA SEARCH

We search for triple systems akin to those required by the collisional-triple model using two approaches: first, by identifying resolved WD binaries with projected separations $< 300 \text{ au}$, and searching their surroundings for tertiaries with projected separations $< 9000 \text{ au}$; and, second, by searching for tertiaries projected within 3000 au of unresolved, double-WD, separation $a \sim 0.1 - 1 \text{ au}$, candidates identified via radial-velocity variations. Our search for triples is conservatively inclusive in several respects. First, by pre-selecting WD binaries, and then asking what fraction of those binaries have a tertiary, we obtain an upper limit on the fraction of *all* WDs

in triples, since not all WDs are in binaries. Second, because of projection effects, some of the selected inner binaries will have physical separations $a > 300 \text{ au}$, and some of the counted tertiaries will be at physical separations beyond the tertiary separation range required by the model. By including all of these systems, we will obtain a conservative upper limit on the true fraction of WDs that are in triples with the architecture required by the model.

2.1 Resolved *Gaia* triples

Following [Gentile Fusillo et al. \(2019\)](#), we start by identifying all WD candidates using an initial colour-magnitude cut in *Gaia* DR2 data:

$$\text{parallax_over_error} > 1 \quad (1)$$

$$M_G > 5 \quad (2)$$

$$M_G > 5.93 + 5.047 \times (G_{\text{BP}} - G_{\text{RP}}) \quad (3)$$

$$M_G > 6 \times (G_{\text{BP}} - G_{\text{RP}})^3 + \\ - 21.77 \times (G_{\text{BP}} - G_{\text{RP}})^2 + \\ + 27.91 \times (G_{\text{BP}} - G_{\text{RP}}) + 0.897 \quad (4)$$

$$(G_{\text{BP}} - G_{\text{RP}}) < 1.7 \quad (5)$$

where $M_G = \text{phot_g_mean_mag} + 5 \times \log_{10}(\text{parallax}) - 10$ is the absolute magnitude in the *G* band. This results in 8,144,732 sources. We further select only those within a distance of 120 pc:

$$\text{parallax} > 8.33 \quad (6)$$

leaving 313,871 sources. We follow [Gaia Collaboration et al. \(2018b\)](#) and remove astrometric artefacts by requiring:

$$\sqrt{\frac{\chi^2}{\nu' - 5}} < 1.2 \max\left(1, e^{-0.2(G-19.5)}\right) \quad (7)$$

where χ^2 is `astrometric_chi2_al` and ν' is `astrometric_n_good_obs_al` in the *Gaia* database, leaving 86,182 sources.

Since the G_{BP} and G_{RP} fluxes are calculated by integrating over low-resolution spectra, they are more prone to contamination from nearby sources, compared to the *G*-band flux, which is measured by photometric profile fitting. Following [El-Badry & Rix \(2018\)](#) and [Evans et al. \(2018\)](#), we filter out sources that might be contaminated by nearby sources by limiting the total G_{BP} and G_{RP} excess compared to the *G* band:

$$\text{phot_bp_rp_excess_factor} > 1.0 + 0.015(G_{\text{BP}} - G_{\text{RP}})^2 \quad (8)$$

$$\text{phot_bp_rp_excess_factor} < 1.3 + 0.06(G_{\text{BP}} - G_{\text{RP}})^2 \quad (9)$$

leaving 26,591 sources.

We further follow [El-Badry & Rix \(2018\)](#) by selecting only sources with high signal-to-noise ratio photometry, i.e., < 2 per cent flux uncertainty in the *G* band, and < 5 per cent in both the G_{BP} and G_{RP} bands:

$$\text{phot_g_mean_flux_over_error} > 50 \quad (10)$$

$$\text{phot_rp_mean_flux_over_error} > 20 \quad (11)$$

$$\text{phot_bp_mean_flux_over_error} > 20 \quad (12)$$

leaving 17,410 sources. These criteria assure that we only select sources that fall with high certainty within in the WD region of the colour-magnitude diagram.

Finally, we select only sources where the relative error on the parallax is smaller than 10 per cent:

$$\text{parallax_over_error} > 10 \quad (13)$$

resulting in 17,395 sources.

We then choose all physical-double resolved WDs within 120 pc with projected separations < 300 au, by requiring

$$\frac{\theta}{\text{arcsec}} \leq 10^{-3} \frac{s}{\text{au}} \frac{\varpi}{\text{mas}} \quad (14)$$

where θ is the angular separation, $s = 300$ au is the projected separation, and ϖ is the parallax. Following El-Badry & Rix (2018, eq. 2) we further select only pairs with consistent parallaxes:

$$\Delta d - 2s \leq 3\sigma_{\Delta d}, \quad (15)$$

where $\Delta d = |1/\varpi_1 - 1/\varpi_2|$ pc, $s = \theta/\varpi_1$ pc, and $\sigma_{\Delta d} = \sqrt{\sigma_{\varpi,1}^2/\varpi_1^4 + \sigma_{\varpi,2}^2/\varpi_2^4}$ pc. Here ϖ_i and $\sigma_{\varpi,i}$ are the parallax of the i th target and its standard error in arcsec, respectively, and the angular separation, θ , is in radians. This means that we inclusively count a system as a WD binary, even if its component distances differ at the $3\sigma_{\Delta d}$ level.

The search results in 27 WD pairs, listed in Table 1, out of the 17,395 WDs that are nearer than 120 pc. The relative projected velocity differences between the members of each pair, also listed in Table 1, are well below the $\sim 6 \text{ km s}^{-1}$ maximum that is possible between bound solar-mass objects, indicating these are real, bound, pairs. Fig. 1 shows the WD-pair locations on the *Gaia* colour-magnitude diagram.

We note, following El-Badry & Rix (2018) and Arenou et al. (2018), that the above 27 resolved pairs are a small fraction of the actual number of WD pairs with separations < 300 au, which is likely to be at least 10 per cent (Maoz et al. 2018). First, *Gaia* is incomplete to binaries at angular separations $\theta \lesssim 0.7''$, corresponding to 84 au at 120 pc. More importantly, the *Gaia* $G_{BP} - G_{RP}$ colour is not available, in most cases, for both components of doubles with projected separations $\theta < 2''$ (240 au at 120 pc), selecting against the identification of one or both stars as WDs. We further note that extending the WD sample to 200 or 300 pc did not result in any additional < 300 au WD pairs, likely because of the limitations imposed by the resolution, which become more severe with distance. However, our strategy for testing the collisional-triple model does not require a complete census of WD binaries; to the contrary, we select only a small minority of double-WDs that *Gaia* can detect, but then perform a thorough search for tertiaries around these binaries.

By limiting our sample of WD pairs to 120 pc, we expect that, at the limiting *Gaia* magnitude $G \sim 20$, we are sensitive and largely complete to tertiary companions corresponding to the faintest, lowest-mass, main-sequence stars, as well as the coolest WDs. As shown by Gentile Fusillo et al. (2019, fig. 19), the 100 pc *Gaia* DR2 WD sample is complete up to $M_G \sim 16$, indeed corresponding to all but the coolest few percent of WDs with $M_G > 16$ (Isern 2019; Tremblay et al. 2019). This completeness likely applies also at the relatively brighter luminosities near the bottom of the main sequence ($M_G \sim 14$, $T_{\text{eff}} \lesssim 3000$ K), corresponding to $\lesssim 0.2 M_{\odot}$ M-dwarfs (Hillenbrand & White 2004). However, a more thorough future assessment of the main-sequence completeness at 120 pc will place our conclusions, below, on a surer footing.

Next, we search for tertiary companions around the inner double WDs, by querying the entire *Gaia* DR2 database. Assuming a uniform distribution of orbital eccentricities, as supported by observations (Duchêne & Kraus 2013; Tokovinin & Kiyaveva 2016), the mean eccentricity is $\langle e \rangle = 1/2$, and the apocentre separation is

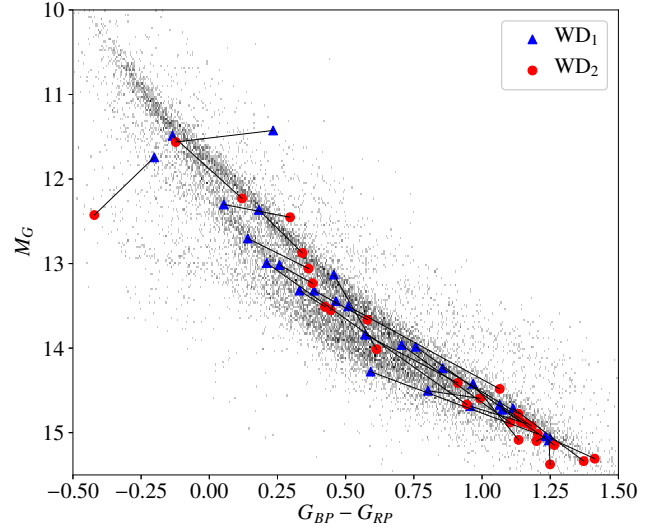


Figure 1. *Gaia* colour-magnitude diagram for resolved double WDs within 120 pc, with projected separations $s < 300$ au. Pairs are connected by black solid lines, where the photometric primary (secondary) is marked by a blue triangle (red circle). None of the pairs have a tertiary companion with a projected separation $s < 9000$ au. The number density in this parameter space of the full 120 pc WD sample from *Gaia* (17,395 sources) is shown in grayscale for reference.

therefore, on average, $(1+e)/(1-e) = 3$ times the pericentre separation. The apocentre separation of the tertiary star in the collisional model can thus be as high as $\sim 30a$, and we therefore search for tertiaries projected within 9000 au of the inner, $a < 300$ au, double WDs.

For the tertiaries we include sources only if they satisfy $\text{parallax_over_error} > 5$, Eq. 7 (astrometric artefacts removal), and Eq. 15 (distance from the first WD in the inner binary), but this time we allow only a $2\sigma_{\Delta d}$ difference in the distances. None of the 27 resolved inner WD binaries has a candidate tertiary companion projected within 9000 au. With Poisson statistics, this null detection implies, at 95 per cent confidence, the existence of < 3 tertiaries, or an upper limit of < 11 per cent on the fraction of $a < 300$ au-separation double WDs with a tertiary companion with $r_{\text{peri,out}} = (3-10)a$.

2.2 *Gaia* tertiaries to SPY double WDs

To further explore the potential triple SN Ia progenitor landscape, we have searched for tertiaries around a second sample of close double-WD binaries, this time unresolved WD binary candidates from the Supernova Progenitor survey (SPY; Napiwotzki et al. 2001). The SPY survey was a few-epoch spectroscopic survey of ~ 800 bright ($V \sim 16$ mag) WDs conducted with the European Southern Observatory 8 m Very Large Telescope, with the objective of using radial-velocity differences between epochs to identify close double-WD systems that will merge within a Hubble time. In Maoz & Hallakoun (2017) we measured the maximal changes in radial velocity (ΔRV_{max}) between epochs, and modelled the observed ΔRV_{max} statistics via Monte Carlo simulations (Maoz et al. 2012; Badenes & Maoz 2012), to constrain the population characteristics of double WDs. We identified 43 high- ΔRV_{max} systems as likely double-WD candidates (see table 1 of Maoz & Hallakoun 2017),

Table 1. Resolved double WDs within 120 pc, with projected separations $s < 300$ au. Each system appears as a pair of rows separated by a line. Columns give *Gaia* DR2 ID, parallax, distance, and proper motion. The third row of each system lists its angular and projected separations, and the relative proper motion. None of these WD pairs have a tertiary star within a projected separation of 9000 au.

GaiaID	ϖ (mas)	d (pc)	μ_{RA} (mas yr $^{-1}$)	μ_{Dec} (mas yr $^{-1}$)	v_{RA} (km s $^{-1}$)	v_{Dec} (km s $^{-1}$)
4617812054836337536	17.83 ± 0.19	56.07 ± 0.60	58.55 ± 0.41	-190.23 ± 0.33	15.56 ± 0.20	-50.56 ± 0.55
4617812054837799168	18.12 ± 0.17	55.19 ± 0.52	57.93 ± 0.36	-191.60 ± 0.29	15.16 ± 0.17	-50.13 ± 0.48
		$\theta = 3.92450 \pm 0.00011''$	$s = 220.1 \pm 2.4$ au		$v_{\text{rel}} = 0.60 \pm 0.69$ km s $^{-1}$	
2482813425794003200	23.94 ± 0.19	41.77 ± 0.33	-264.84 ± 0.38	-265.05 ± 0.17	-52.45 ± 0.43	-52.49 ± 0.42
2482813430089468160	23.36 ± 0.19	42.80 ± 0.35	-259.72 ± 0.38	-264.77 ± 0.16	-52.70 ± 0.43	-53.72 ± 0.44
		$\theta = 3.18446 \pm 0.00022''$	$s = 133.0 \pm 1.1$ au		$v_{\text{rel}} = 1.26 \pm 0.71$ km s $^{-1}$	
4613612951211823616	33.859 ± 0.036	29.534 ± 0.032	-61.767 ± 0.062	-22.360 ± 0.056	-8.648 ± 0.013	-3.1306 ± 0.0086
4613612951211823104	33.848 ± 0.047	29.543 ± 0.041	-73.700 ± 0.078	-11.815 ± 0.072	-10.322 ± 0.018	-1.655 ± 0.010
		$\theta = 7.127628 \pm 0.000039''$	$s = 210.51 \pm 0.22$ au		$v_{\text{rel}} = 2.232 \pm 0.017$ km s $^{-1}$	
16166875378033664	10.16 ± 0.19	98.4 ± 1.9	55.98 ± 0.32	-60.44 ± 0.27	26.12 ± 0.51	-28.20 ± 0.55
16166875377576064	10.59 ± 0.35	94.4 ± 3.1	56.62 ± 0.57	-58.12 ± 0.48	25.34 ± 0.88	-26.01 ± 0.89
		$\theta = 2.94598 \pm 0.00029''$	$s = 290.0 \pm 5.5$ au		$v_{\text{rel}} = 2.3 \pm 1.3$ km s $^{-1}$	
3249479592235301376	32.16 ± 0.11	31.10 ± 0.10	-28.35 ± 0.18	-262.86 ± 0.19	-4.179 ± 0.029	-38.75 ± 0.13
3249479592234269056	32.25 ± 0.13	31.01 ± 0.13	-8.52 ± 0.22	-264.95 ± 0.25	-1.252 ± 0.033	-38.95 ± 0.16
		$\theta = 5.40038 \pm 0.00012''$	$s = 167.93 \pm 0.55$ au		$v_{\text{rel}} = 2.933 \pm 0.042$ km s $^{-1}$	
3404213863614488192	10.70 ± 0.13	93.5 ± 1.2	-18.61 ± 0.21	19.61 ± 0.16	-8.25 ± 0.14	8.69 ± 0.13
3404213863611804672	10.73 ± 0.12	93.2 ± 1.1	-17.53 ± 0.20	17.31 ± 0.15	-7.74 ± 0.12	7.65 ± 0.11
		$\theta = 3.09811 \pm 0.00014''$	$s = 289.6 \pm 3.6$ au		$v_{\text{rel}} = 1.16 \pm 0.21$ km s $^{-1}$	
3001062974507933952	16.85 ± 0.25	59.36 ± 0.89	-163.00 ± 0.37	-75.65 ± 0.46	-45.87 ± 0.70	-21.29 ± 0.34
3001062974507934080	16.59 ± 0.28	60.3 ± 1.0	-168.99 ± 0.42	-75.74 ± 0.50	-48.29 ± 0.83	-21.65 ± 0.39
		$\theta = 4.35293 \pm 0.00033''$	$s = 258.4 \pm 3.9$ au		$v_{\text{rel}} = 2.5 \pm 1.1$ km s $^{-1}$	
3144837318276010624	54.935 ± 0.070	18.203 ± 0.023	211.54 ± 0.13	-1782.658 ± 0.077	18.255 ± 0.026	-153.83 ± 0.20
3144837112117580800	55.141 ± 0.061	18.135 ± 0.020	209.90 ± 0.11	-1790.484 ± 0.063	18.045 ± 0.022	-153.93 ± 0.17
		$\theta = 16.404756 \pm 0.000064''$	$s = 298.62 \pm 0.38$ au		$v_{\text{rel}} = 0.231 \pm 0.082$ km s $^{-1}$	
1118460924702185088	21.83 ± 0.15	45.80 ± 0.31	-227.50 ± 0.17	-315.27 ± 0.22	-49.40 ± 0.34	-68.45 ± 0.47
1118460924703171584	21.60 ± 0.11	46.29 ± 0.24	-224.95 ± 0.12	-311.65 ± 0.17	-49.36 ± 0.26	-68.39 ± 0.36
		$\theta = 3.53694 \pm 0.00012''$	$s = 162.0 \pm 1.1$ au		$v_{\text{rel}} = 0.07 \pm 0.72$ km s $^{-1}$	
606938634805314944	17.817 ± 0.077	56.13 ± 0.24	-115.21 ± 0.13	-26.764 ± 0.097	-30.65 ± 0.14	-7.121 ± 0.040
606938634805314816	17.747 ± 0.066	56.35 ± 0.21	-115.58 ± 0.11	-22.206 ± 0.076	-30.87 ± 0.12	-5.931 ± 0.030
		$\theta = 3.765706 \pm 0.000069''$	$s = 211.36 \pm 0.91$ au		$v_{\text{rel}} = 1.210 \pm 0.034$ km s $^{-1}$	
798602271945568256	14.54 ± 0.20	68.79 ± 0.96	8.81 ± 0.40	-104.02 ± 0.47	2.87 ± 0.14	-33.92 ± 0.50
798602267650286464	13.68 ± 0.40	73.1 ± 2.1	10.10 ± 0.79	-108.30 ± 0.93	3.50 ± 0.29	-37.5 ± 1.1
		$\theta = 3.07552 \pm 0.00058''$	$s = 211.6 \pm 3.0$ au		$v_{\text{rel}} = 3.7 \pm 1.2$ km s $^{-1}$	
5436014972680358272	38.082 ± 0.030	26.259 ± 0.021	-339.427 ± 0.036	181.405 ± 0.046	-42.252 ± 0.034	22.581 ± 0.019
5436014972680358784	38.060 ± 0.031	26.275 ± 0.021	-328.220 ± 0.037	167.831 ± 0.048	-40.881 ± 0.033	20.904 ± 0.018
		$\theta = 4.427489 \pm 0.000033''$	$s = 116.262 \pm 0.093$ au		$v_{\text{rel}} = 2.166 \pm 0.050$ km s $^{-1}$	
3970693313784409344	9.74 ± 0.30	102.6 ± 3.2	-62.06 ± 0.49	2.09 ± 0.36	-30.19 ± 0.97	1.02 ± 0.18
3970693313782310656	9.92 ± 0.26	100.8 ± 2.6	-60.16 ± 0.42	2.62 ± 0.31	-28.76 ± 0.77	1.25 ± 0.15
		$\theta = 2.68969 \pm 0.00029''$	$s = 276.1 \pm 8.6$ au		$v_{\text{rel}} = 1.5 \pm 1.2$ km s $^{-1}$	
5874024774146311808	8.69 ± 0.11	115.0 ± 1.5	-33.69 ± 0.15	-53.24 ± 0.18	-18.37 ± 0.25	-29.03 ± 0.39
5874024769842933760	8.424 ± 0.080	118.7 ± 1.1	-33.808 ± 0.099	-54.57 ± 0.11	-19.02 ± 0.19	-30.71 ± 0.30
		$\theta = 2.569850 \pm 0.000056''$	$s = 295.6 \pm 3.9$ au		$v_{\text{rel}} = 1.80 \pm 0.56$ km s $^{-1}$	
5886778250054825344	9.40 ± 0.22	106.4 ± 2.5	-32.52 ± 0.46	-61.25 ± 0.36	-16.40 ± 0.45	-30.89 ± 0.74
5886777494107570176	8.98 ± 0.26	111.3 ± 3.2	-32.25 ± 0.55	-59.38 ± 0.43	-17.01 ± 0.57	-31.33 ± 0.94
		$\theta = 2.78136 \pm 0.00015''$	$s = 295.8 \pm 6.9$ au		$v_{\text{rel}} = 0.8 \pm 1.2$ km s $^{-1}$	
4450425359563998720	11.69 ± 0.13	85.57 ± 0.94	-19.16 ± 0.18	50.88 ± 0.11	-7.77 ± 0.11	20.64 ± 0.23
4450425359563998848	11.58 ± 0.15	86.4 ± 1.1	-18.26 ± 0.21	48.39 ± 0.13	-7.47 ± 0.13	19.81 ± 0.26
		$\theta = 2.61608 \pm 0.00011''$	$s = 223.9 \pm 2.5$ au		$v_{\text{rel}} = 0.88 \pm 0.37$ km s $^{-1}$	
1408135749896104192	25.377 ± 0.027	39.406 ± 0.042	22.799 ± 0.048	-70.057 ± 0.051	4.259 ± 0.010	-13.087 ± 0.017
1408135749896103936	25.342 ± 0.029	39.460 ± 0.044	15.026 ± 0.051	-70.573 ± 0.057	2.811 ± 0.010	-13.201 ± 0.018
		$\theta = 5.611901 \pm 0.000025''$	$s = 221.14 \pm 0.23$ au		$v_{\text{rel}} = 1.453 \pm 0.014$ km s $^{-1}$	

Table 1 – continued

GaiaID	ϖ (mas)	d (pc)	μ_{RA} (mas yr $^{-1}$)	μ_{Dec} (mas yr $^{-1}$)	v_{RA} (km s $^{-1}$)	v_{Dec} (km s $^{-1}$)
2269560710341753728	17.667 ± 0.086	56.60 ± 0.28	-43.88 ± 0.15	-135.61 ± 0.20	-11.774 ± 0.070	-36.39 ± 0.18
2269560710340167296	17.77 ± 0.16	56.26 ± 0.50	-42.37 ± 0.28	-137.58 ± 0.37	-11.30 ± 0.13	-36.69 ± 0.34
	$\theta = 3.22349 \pm 0.00017''$		$s = 182.46 \pm 0.89$ au		$v_{rel} = 0.56 \pm 0.14$ km s $^{-1}$	
2150591795574568192	20.93 ± 0.19	47.78 ± 0.43	-156.56 ± 0.42	-160.73 ± 0.39	-35.46 ± 0.33	-36.40 ± 0.34
2150591799870095872	20.71 ± 0.17	48.29 ± 0.39	-155.79 ± 0.35	-158.73 ± 0.33	-35.66 ± 0.30	-36.34 ± 0.31
	$\theta = 5.51585 \pm 0.00014''$		$s = 263.5 \pm 2.4$ au		$v_{rel} = 0.22 \pm 0.29$ km s $^{-1}$	
4257063458004688896	25.24 ± 0.10	39.63 ± 0.16	118.65 ± 0.20	115.82 ± 0.19	22.287 ± 0.097	21.756 ± 0.095
4257063453704172416	25.131 ± 0.080	39.79 ± 0.13	117.04 ± 0.17	122.90 ± 0.18	22.077 ± 0.077	23.181 ± 0.081
	$\theta = 2.74113 \pm 0.00011''$		$s = 108.62 \pm 0.44$ au		$v_{rel} = 1.44 \pm 0.11$ km s $^{-1}$	
6650228409376970880	16.34 ± 0.30	61.2 ± 1.1	-90.47 ± 0.30	-29.11 ± 0.29	-26.25 ± 0.50	-8.45 ± 0.18
6650228409380791040	16.53 ± 0.12	60.49 ± 0.42	-87.42 ± 0.12	-23.54 ± 0.12	-25.07 ± 0.18	-6.750 ± 0.058
	$\theta = 3.66520 \pm 0.00012''$		$s = 224.3 \pm 4.2$ au		$v_{rel} = 2.07 \pm 0.44$ km s $^{-1}$	
2080526555267049984	34.718 ± 0.072	28.803 ± 0.060	-455.33 ± 0.14	-401.45 ± 0.15	-62.17 ± 0.13	-54.81 ± 0.12
2080526555267050496	34.731 ± 0.061	28.793 ± 0.051	-453.28 ± 0.12	-404.61 ± 0.12	-61.87 ± 0.11	-55.225 ± 0.099
	$\theta = 8.637912 \pm 0.000088''$		$s = 248.80 \pm 0.52$ au		$v_{rel} = 0.510 \pm 0.033$ km s $^{-1}$	
6466132607691464320	20.20 ± 0.23	49.50 ± 0.57	12.38 ± 0.28	-59.52 ± 0.39	2.904 ± 0.074	-13.97 ± 0.18
6466132607693274496	20.06 ± 0.16	49.85 ± 0.39	4.24 ± 0.18	-54.13 ± 0.20	1.002 ± 0.042	-12.79 ± 0.11
	$\theta = 2.11378 \pm 0.00013''$		$s = 104.6 \pm 1.2$ au		$v_{rel} = 2.24 \pm 0.15$ km s $^{-1}$	
1801239293158983168	15.02 ± 0.14	66.58 ± 0.64	-58.22 ± 0.27	-103.72 ± 0.33	-18.37 ± 0.19	-32.73 ± 0.33
1801239297453428992	14.79 ± 0.11	67.63 ± 0.53	-60.42 ± 0.22	-105.84 ± 0.26	-19.37 ± 0.17	-33.93 ± 0.28
	$\theta = 3.16333 \pm 0.00013''$		$s = 210.6 \pm 2.0$ au		$v_{rel} = 1.56 \pm 0.48$ km s $^{-1}$	
2841680934336159104	21.76 ± 0.24	45.96 ± 0.50	-85.16 ± 0.32	-179.28 ± 0.22	-18.56 ± 0.21	-39.06 ± 0.42
2841680934336158976	21.70 ± 0.14	46.09 ± 0.30	-72.14 ± 0.22	-177.52 ± 0.14	-15.76 ± 0.11	-38.79 ± 0.25
	$\theta = 3.71565 \pm 0.00013''$		$s = 170.8 \pm 1.8$ au		$v_{rel} = 2.81 \pm 0.28$ km s $^{-1}$	
1997383581920045312	19.96 ± 0.16	50.09 ± 0.41	128.12 ± 0.22	62.29 ± 0.18	30.42 ± 0.26	14.79 ± 0.13
1997383581913649152	19.95 ± 0.15	50.12 ± 0.37	135.64 ± 0.20	68.36 ± 0.16	32.23 ± 0.24	16.24 ± 0.13
	$\theta = 2.41721 \pm 0.00010''$		$s = 121.1 \pm 1.0$ au		$v_{rel} = 2.31 \pm 0.38$ km s $^{-1}$	
2017484922210746368	17.68 ± 0.26	56.57 ± 0.83	346.07 ± 0.49	211.20 ± 0.36	92.8 ± 1.4	56.63 ± 0.84
2017484922214792576	17.33 ± 0.12	57.69 ± 0.40	344.68 ± 0.20	209.45 ± 0.17	94.26 ± 0.65	57.28 ± 0.40
	$\theta = 2.63999 \pm 0.00020''$		$s = 149.3 \pm 2.2$ au		$v_{rel} = 1.6 \pm 1.8$ km s $^{-1}$	

and an additional double-lined system that was not included in the candidate list because of its low ΔRV_{max} (HE 0315–0118).

Since the *Gaia* DR2 astrometric model does not take binarity and potential astrometric wobble into account, it might fail, or not fail, but report spurious results in case of unresolved binaries (e.g. Hollands et al. 2018). We have verified that full five-parameter astrometric solutions are reported for all 44 SPY systems. To further check for spurious distances, we compared the astrometric distances derived from *Gaia*'s parallaxes with the photometric distances for these WDs. We used the spectroscopic effective temperatures and surface gravities derived by Koester et al. (2009) to generate synthetic WD model spectra using the spectral synthesis program SYN-SPEC (version 50; Hubeny & Lanz 2011), based on model atmospheres created by the TLUSTY program (version 205; Hubeny 1988; Hubeny & Lanz 1995, 2017). The luminosities were then estimated by assuming a mass-radius relation ('thick' hydrogen-dominated carbon-oxygen WD cooling tracks² from Fontaine et al. 2001). Finally, the photometric distances were calculated using the *V/B*-band magnitudes reported in Koester et al. (2009). We find that the photometric distances of all of the SPY WDs are consistent with their

Gaia distances, with a scatter ~ 10 per cent, and with few or no obvious outliers that could be indicative of spurious *Gaia* distances. Nonetheless, future *Gaia* data releases that will include binarity in the astrometric model are required in order to verify that none of the WD distances are erroneous due to unresolved binarity.

As with the previous sample, we have searched with *Gaia* for tertiaries within 3000 au of these 44 candidate close-double-WDs from SPY. Contrary to the previous sample, the triple systems turned up here are not actual candidate progenitors for the collisional-triple scenario, since their inner separations are of order 0.1–4 au, whereas the tertiary separation is of order 10^{3-4} larger, rather than just 3–30 times larger, as required by the model. The tertiaries within only 120 au, which would be have been relevant to the model, are well below the *Gaia* angular resolution limit at the typical distances of the SPY WDs (~ 10 –250 pc). Nevertheless, it is instructive to estimate the frequency of these "extreme" (rather than "mild") hierarchical triples, to learn about the triple population in this different hierarchy range.

Among the 44 SPY double-WD candidates, we find four with tertiaries projected within < 3000 au separation, satisfying $parallax_over_error > 5$, Eq. 7 (astrometric artefacts removal), and Eq. 15 (distance from the first WD in the inner binary, within $2\sigma_{\Delta d}$). We list them in Table 2. Their location on the *Gaia* colour-

² <http://www.astro.umontreal.ca/bergeron/CoolingModels/>

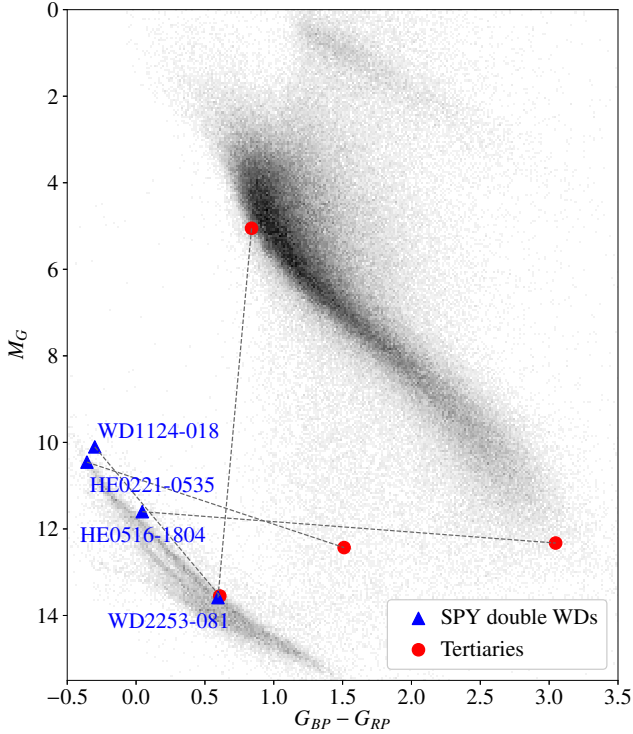


Figure 2. Candidate unresolved double WDs from the SPY sample (blue triangles) with a tertiary stellar companion in *Gaia* with projected separations $s < 3000$ au (red circles). Pairs are connected by dashed lines. The number density of stars from a random *Gaia* sample and the full 120 pc WD sample is shown in grayscale.

magnitude diagram is shown in Fig. 2. At 3000 au separation, the maximum velocity difference due to orbital motion is $\sim 1.5 \text{ km s}^{-1}$, and again all four candidate tertiaries are consistent with a velocity difference that is lower than this, arguing that these are true bound systems. The M-dwarf tertiary we find for HE 0516–1804 could be the source of the infrared excess we found in its photometry in Maoz & Hallakoun (2017). We note that the known M-dwarf tertiary candidate of WD 0326–273 (Nelemans et al. 2005, and references therein) failed to pass our consistent parallax criterion (Eq. 15), with $\sigma_{\Delta d} \sim 5$.

This result suggests that $\lesssim 9$ per cent of separation- $a \sim 0.1 - 4$ au double WDs have tertiaries within separations of 3000 au. Again, the population of tertiaries considered around this sample is much more extensive than those with a role in the collisional-triple SN Ia model.

3 DISCUSSION

We have used *Gaia* to search for candidate triple stellar systems similar to those envisaged in the collisional triple SN Ia progenitor model, and to assess their abundance. *Gaia*, due to its angular resolution limits, is strongly biased against detection of the separation $a < 300$ au inner WD binaries of the proposed triple systems. We have therefore focused on two samples of “known” double WDs, and used *Gaia* to search for a putative wide tertiary member out to 9000 au separations, where *Gaia* completeness is high. Our first inner-double-WD sample consists of 27 WD pairs with projected separations $s < 300$ au, found in the *Gaia* DR2 database among

$\sim 17,400$ WDs within a 120 pc distance. These 27 systems are the small fraction of the actual number of double WDs having such separations that are detected as binaries, because of *Gaia*’s low sensitivity in this regime.

Around this sample of 27 *Gaia*-selected inner-WD-binaries, we find no tertiary stars of any kind (WD or main-sequence, down to the lowest stellar masses) out to 9000 au projected separations. Such systems, had they been found, could correspond closely in separation and hierarchy to the SN Ia progenitors in the model. Their non-detection sets a 95 per-cent-confidence upper limit of 11 per cent on the fraction of $a < 300$ au WD binaries that are orbited by a tertiary with pericentre separation 3 – 10 times the inner-binary separation. Maoz et al. (2018) have combined the ΔRV_{max} results of Badenes & Maoz (2012) and Maoz & Hallakoun (2017), to deduce that the fraction of WDs in binaries in the range 0.01 to 4 au is 10 ± 2.5 per cent, with a separation distribution in this range consistent with a power law, a^α , with $\alpha = -1.3 \pm 0.2$. El-Badry & Rix (2018), analysing the resolved binary WD population that they find with *Gaia*, and after accounting for selection and incompleteness effects, find a power-law separation distribution with a slope, again, close to $\alpha = -1$ (i.e. equal numbers per logarithmic interval in separation) in the range $a = 50 - 1500$ au. Considering then that there is a similar number of decades in separation between 0.01 – 4 au (Maoz et al. 2018) and between 1 – 300 au (the range of inner-binary separations in the Katz & Dong (2012) model), implies that ~ 10 per cent of all WDs are in binaries with $a = 1 - 300$ au. Combined with our present result that, at most, 11 per cent of such binaries host a tertiary companion out to 9000 au, we conclude that the fraction among WDs of triple systems with the architecture required by the collisional-triple model is < 1 per cent, at the 95 per cent confidence level. This triple fraction is at least a factor $\sim 30 - 55$ times lower than the fraction required by the model ($\sim 30 - 55$ per cent, see Section 1).

A second double-WD sample that we have studied consists of 44 unresolved, separation $a \sim 0.1 - 4$ au candidate WD binaries that have emerged, based on radial-velocity variations, from SPY. We searched the SPY candidate WD binaries for tertiary companions, this time out to 3000 au separations, i.e., a much larger range than relevant for the collisional model. Here, we found four candidate tertiary companions (two main-sequence stars, a WD, and an uncertain case, perhaps a subdwarf) with actual projected separations from 190 to 1650 au. Considering the WD binarity fraction of roughly 4 per cent for every decade of separation (see above), the 9 per cent fraction of tertiaries (of all kinds) in this separation range around short-orbit WD binaries is not surprising. Combined with the abundance of inner-WD binaries, we again get a 1 per cent upper limit on the fraction of WDs that are in triples, consisting of an inner double WD plus a tertiary (although now triples of a different hierarchy than those required by the collisional-triple model).

We conclude that there is at least a 1.5 order of magnitude deficit, and likely more, in the fraction of WDs that are in the types of triple systems required by the collisional-triple model. The double WDs in our first, $s < 300$ au, sample have actual separations in the 100 – 300 au range. A remaining “hiding place” for the progenitor systems of the model could be in the unexplored parameter range of $a \sim 1 - 100$ au WD binaries. A large fraction of all WDs would need to be in binaries with this separation range, and a large fraction of those same binaries would need to have tertiaries at separations $(3 - 10)a$. The first condition is unlikely to be true, given the similar separation distributions (about flat in log separation, see above) followed by binary WDs within the $a = 0.01 - 4$ au range and the $a = 50 - 1500$ au range. The second condition is also unlikely, given

Table 2. Candidate unresolved double-WD systems from the SPY sample having a *Gaia* tertiary companion with projected separation $s < 3000$ au. Each triple system appears as a pair of rows separated by a line. The first line of each pair represents the inner (unresolved) double WD, and the second line describes the tertiary star. Columns as in Table 1.

Name	GaiaID	ϖ (mas)	d (pc)	μ_{RA} (mas yr ⁻¹)	μ_{Dec} (mas yr ⁻¹)	v_{RA} (km s ⁻¹)	v_{Dec} (km s ⁻¹)
HE0221-0535	2488754366292015744	8.97 ± 0.11	111.5 ± 1.3	-17.85 ± 0.13	5.69 ± 0.12	-9.43 ± 0.13	3.006 ± 0.075
	2488754366292015872	8.40 ± 0.29	119.0 ± 4.1	-18.72 ± 0.33	5.97 ± 0.28	-10.56 ± 0.41	3.37 ± 0.20
		$\theta = 2.68970 \pm 0.00019''$		$s = 299.8 \pm 3.6$ au		$v_{rel} = 1.19 \pm 0.45$ km s ⁻¹	
HE0516-1804	2981590730954538112	11.884 ± 0.061	84.15 ± 0.43	9.90 ± 0.10	-30.24 ± 0.11	3.951 ± 0.046	-12.061 ± 0.077
	2981590730954537984	11.679 ± 0.099	85.63 ± 0.72	11.17 ± 0.16	-31.72 ± 0.18	4.535 ± 0.076	-12.87 ± 0.13
		$\theta = 2.289622 \pm 0.000094''$		$s = 192.66 \pm 0.99$ au		$v_{rel} = 1.00 \pm 0.15$ km s ⁻¹	
WD1124-018	3796545519645331584	5.47 ± 0.11	182.8 ± 3.8	-35.87 ± 0.18	11.95 ± 0.12	-31.08 ± 0.66	10.36 ± 0.24
	3796545515349746432	5.84 ± 0.70	171 ± 21	-35.66 ± 0.98	11.64 ± 0.63	-29.0 ± 3.6	9.5 ± 1.2
		$\theta = 9.01849 \pm 0.00056''$		$s = 1649 \pm 34$ au		$v_{rel} = 2.3 \pm 3.8$ km s ⁻¹	
WD2253-081	2610488514148351360	27.78 ± 0.11	35.99 ± 0.14	549.25 ± 0.13	-46.94 ± 0.12	93.71 ± 0.36	-8.009 ± 0.037
	2610488514148352000	27.732 ± 0.075	36.060 ± 0.097	551.706 ± 0.090	-48.924 ± 0.084	94.31 ± 0.25	-8.363 ± 0.027
		$\theta = 41.656756 \pm 0.000075''$		$s = 1499.3 \pm 5.7$ au		$v_{rel} = 0.69 \pm 0.40$ km s ⁻¹	

the rarity of tertiary stars around WD binaries with those separation ranges, as shown here. A different progenitor and explosion scenario is most probably at the root of SN Ia explosions.

ACKNOWLEDGEMENTS

We thank Boaz Katz, Julio Chanamé, J. J. Hermes, and the anonymous referee for valuable comments. This work was supported by a grant from the Israel Science Foundation (ISF). This work has made use of data from the European Space Agency (ESA) mission *Gaia* (<https://www.cosmos.esa.int/gaia>), processed by the *Gaia* Data Processing and Analysis Consortium (DPAC, <https://www.cosmos.esa.int/web/gaia/dpac/consortium>). Funding for the DPAC has been provided by national institutions, in particular the institutions participating in the *Gaia* Multilateral Agreement.

This research made use of `ASTROPY`³, a community-developed core PYTHON package for Astronomy ([Astropy Collaboration et al. 2013, 2018](https://www.astropy.org)), `ASTROQUERY` ([Ginsburg et al. 2013](https://www.astropy.org)), `MATPLOTLIB` ([Hunter 2007](https://matplotlib.org/)), `NUMPY` ([Oliphant 2006; van der Walt et al. 2011](https://numpy.org/)), `UNCERTAINTIES`⁴, a PYTHON package for calculations with uncertainties by Eric O. Lebigot, and `TOPCAT` ([Taylor 2005](https://www.starlink.rl.ac.uk/)), a tool for operations on catalogues and tables.

REFERENCES

Arenou F., et al., 2018, *A&A*, **616**, A17
 Astropy Collaboration et al., 2013, *A&A*, **558**, A33
 Astropy Collaboration et al., 2018, *AJ*, **156**, 123
 Badenes C., Maoz D., 2012, *ApJ*, **749**, L11
 Benz W., Hills J. G., Thielemann F. K., 1989, *ApJ*, **342**, 986
 De Rosa R. J., et al., 2014, *MNRAS*, **437**, 1216
 Dong S., Katz B., Kushnir D., Prieto J. L., 2015, *MNRAS*, **454**, L61
 Dong S., et al., 2018, *MNRAS*, **479**, L70
 Duchêne G., Kraus A., 2013, *ARA&A*, **51**, 269
 El-Badry K., Rix H.-W., 2018, *MNRAS*, **480**, 4884

³ <http://www.astropy.org>

⁴ <http://pythonhosted.org/uncertainties/>

Evans D. W., et al., 2018, *A&A*, **616**, A4
 Fontaine G., Brassard P., Bergeron P., 2001, *PASP*, **113**, 409
 Gaia Collaboration et al., 2016, *A&A*, **595**, A1
 Gaia Collaboration et al., 2018a, *A&A*, **616**, A1
 Gaia Collaboration et al., 2018b, *A&A*, **616**, A10
 Gentile Fusillo N. P., et al., 2019, *MNRAS*, **482**, 4570
 Ginsburg A., et al., 2013, *Astroquery* v0.1, [doi:10.6084/m9.figshare.805208.v2](https://doi.org/10.6084/m9.figshare.805208.v2), https://figshare.com/articles/Astroquery_v0_1/805208/2
 Graur O., Bianco F. B., Modjaz M., Shivers I., Filippenko A. V., Li W., Smith N., 2017, *ApJ*, **837**, 121
 Hamers A. S., Pols O. R., Claeys J. S. W., Nelemans G., 2013, *MNRAS*, **430**, 2262
 Hillenbrand L. A., White R. J., 2004, *ApJ*, **604**, 741
 Hollands M. A., Tremblay P. E., Gänsicke B. T., Gentile-Fusillo N. P., Toonen S., 2018, *MNRAS*, **480**, 3942
 Hubeny I., 1988, *Computer Physics Communications*, **52**, 103
 Hubeny I., Lanz T., 1995, *ApJ*, **439**, 875
 Hubeny I., Lanz T., 2011, *Synspec: General Spectrum Synthesis Program*, Astrophysics Source Code Library (ascl:1109.022)
 Hubeny I., Lanz T., 2017, preprint, ([arXiv:1706.01859](https://arxiv.org/abs/1706.01859))
 Hunter J. D., 2007, *Computing In Science & Engineering*, **9**, 90
 Isern J., 2019, *ApJ*, **878**, L11
 Katz B., Dong S., 2012, The rate of WD-WD head-on collisions may be as high as the SNe Ia rate ([arXiv:1211.4584](https://arxiv.org/abs/1211.4584))
 Klein Y. Y., Katz B., 2017, *MNRAS*, **465**, L44
 Koester D., Voss B., Napiwotzki R., Christlieb N., Homeier D., Lisker T., Reimers D., Heber U., 2009, *A&A*, **505**, 441
 Kollmeier J. A., et al., 2019, H- α emission in the nebular spectrum of the Type Ia supernova ASASSN-18tb ([arXiv:1902.02251](https://arxiv.org/abs/1902.02251))
 Kushnir D., Katz B., Dong S., Livne E., Fernández R., 2013, *ApJ*, **778**, L37
 Leigh N. W. C., Geller A. M., 2013, *MNRAS*, **432**, 2474
 Li W., Chornock R., Leaman J., Filippenko A. V., Poznanski D., Wang X., Ganeshalingam M., Mannucci F., 2011, *MNRAS*, **412**, 1473
 Livio M., Mazzali P., 2018, *Phys. Rep.*, **736**, 1
 Maoz D., Hallakoun N., 2017, *MNRAS*, **467**, 1414
 Maoz D., Badenes C., Bickerton S. J., 2012, *ApJ*, **751**, 143
 Maoz D., Mannucci F., Nelemans G., 2014, *ARA&A*, **52**, 107
 Maoz D., Hallakoun N., Badenes C., 2018, *MNRAS*, **476**, 2584
 McMillan P. J., 2011, *MNRAS*, **414**, 2446
 Mermilliod J.-C., Andersen J., Latham D. W., Mayor M., 2007, *A&A*, **473**, 829
 Moe M., Di Stefano R., 2017, *ApJS*, **230**, 15

- Napiwotzki R., et al., 2001, *Astronomische Nachrichten*, 322, 411
- Nelemans G., et al., 2005, *A&A*, 440, 1087
- Oliphant T., 2006, NumPy: A guide to NumPy, USA: Trelgol Publishing, <http://www.numpy.org/>
- Papish O., Perets H. B., 2016, *ApJ*, 822, 19
- Taylor M. B., 2005, in Shopbell P., Britton M., Ebert R., eds, *Astronomical Society of the Pacific Conference Series Vol. 347, Astronomical Data Analysis Software and Systems XIV*. p. 29
- Thompson T. A., 2011, *ApJ*, 741, 82
- Tokovinin A., 2014, *AJ*, 147, 87
- Tokovinin A., Kiyaveva O., 2016, *MNRAS*, 456, 2070
- Tokovinin A., Thomas S., Sterzik M., Udry S., 2008, in Hubrig S., Petrotzens M., Tokovinin A., eds, *Multiple Stars Across the H-R Diagram*. p. 129, doi:10.1007/978-3-540-74745-1_19
- Toonen S., Perets H. B., Hamers A. S., 2018, *A&A*, 610, A22
- Tremblay P.-E., et al., 2019, *Nature*, 565, 202
- Vallely P. J., Tucker M. A., Shappee B. J., Brown J. S., Stanek K. Z., Kochanek C. S., 2019, *Signatures of Bimodality in Nebular Phase Type Ia Supernova Spectra: Indications of White Dwarf Collision Progenitors* ([arXiv:1902.00037](https://arxiv.org/abs/1902.00037))
- Wang B., 2018, *Research in Astronomy and Astrophysics*, 18, 049
- van der Walt S., Colbert S. C., Varoquaux G., 2011, *Computing in Science Engineering*, 13, 22

This paper has been typeset from a $\text{\TeX}/\text{\LaTeX}$ file prepared by the author.